Table I. Calculated Heats of Reaction and Activation Enthalpies for Rearrangement of **1**.

Product formed	Enthalpy, kcal/mol			
	MINDO/3		STO-3G[a]	
	ΔH	$\Delta H^{\ddagger}$	ΔH	$\Delta H^{\ddagger}$
2	−2	50.3	−15.3	97.7
3	−16	42.9	−30.4	56.0
8	−36	23.6	−66.6	9.6

[a] STO-3G energies of **2**, **3**, and **8** are from ref 5. All other STO-3G values were calculated using the geometries in Figure 1.

with mass spectra corresponding to that of an adduct of **3** with methanol.

The known rearrangement of bicyclobutanylidene to **8**[14] has led a referee to suggest an alternative mechanism for the formation of vinylacetylene involving the addition of carbon atoms to the double bond (eq 3). However, the decomposition of [^{14}C]-**5**[9] in the presence of **7** leads to **8** whose specific activity

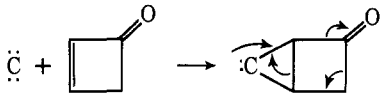

$$\longrightarrow H{-}C{\equiv}C{-}CH{=}CH_2 + CO \quad (3)$$

is only 4% that of starting tetrazole. Hence, the pathway shown in eq 3 cannot account for more than 4% of the vinylacetylene in this system. This result serves to emphasize the known tendency of atomic carbon to react at the point of highest electron density.[12]

Hence, it appears that rearrangement to vinylacetylene is the most favorable pathway for carbene **1**. To explain the reactivity of **1**, we have carried out MINDO/3[15,16] semiempirical molecular orbital calculations of the reaction coordinates for the formation of **2**, **3**, and **8** from **1**; a MINDO/3 study of **2** has been reported by Dewar and Kollmar.[17] The calculated equilibrium geometry of carbene **1** as well as the geometries of the transition states for the three reactions are shown in Figure 1.

The reaction coordinate for the rearrangement of **1** to **8** was the C(3)-C(4) distance. Lengthening this bond carried the molecule through the transition state in Figure 1b to a point where the C(4)-C(3)-C(2) angle was 85°. At this point the angle was slowly opened to 180° generating the remainder of the reaction coordinate. It is interesting that lengthening the C(3)-C(4) bond results in an immediate increase in the bonding interaction between C(1) and C(3). In other words this rearrangement proceeds via a transition state (rather than an intermediate) resembling bicyclobutene, a process depicted schematically in eq 4.

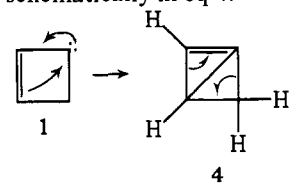

$$\longrightarrow H{-}C{\equiv}C{-}CH{=}CH_2 \quad (4)$$

8

1 **4**

The reaction coordinate for the rearrangement of **1** to **2** is the C(3)-C(4)-H(5) angle. A systematic decrease in this angle carries the molecule over the energy barrier shown in Figure 1c to a nonplanar structure which collapses to **2** when the C(4)-H(5) distance is lengthened. A reaction coordinate for the production of **3** is achieved by lengthening the C(1)-C(4) distance causing the molecule to collapse to **3** via the transition state in Figure 1d.

The calculated heats of reaction and activation enthalpies for these reactions are shown in Table I. As a check on the accuracy of the MINDO/3 results, Table I also lists ab initio STO-3G values for ΔH and $\Delta H^{\ddagger}$. These values were obtained from the STO-3G calculations of Pople and Hehre on **2**, **3**, and **8**[5] and our STO-3G calculations[18] on the molecular geometries shown in Figure 1.

Table I shows that both MINDO/3 and STO-3G calculations rationalize the observed formation of **8** and the absence of **2** and **3** in the rearrangement of **1**. Both the ΔH and the $\Delta H^{\ddagger}$ strongly favor rearrangement of **1** to **8**. This suggests that the exothermicity of the reaction controls product formation. An examination of the Mulliken overlap populations,[19] shown in Figure 1, reveals that bonding in the transition states resembles the bonding in the products rather than the bonding in the starting carbene. Hence, these are late transition states with energies which reflect the heats of formation of the products. This consideration results in the observed rearrangement of **1** to the most thermodynamically stable product.

Acknowledgment. Financial support by the National Science Foundation and by the Research Corporation is gratefully acknowledged.

References and Notes

(1) For leading references see (a) M. Jones, Jr., *Acc. Chem. Res.*, **7**, 415 (1974); (b) C. Wentrup, *Top. Curr. Chem.*, **62**, 173, (1976); (c) W. M. Jones and U. H. Brinker in "Pericyclic Reactions", Vol. I, A. P. Marchand and R. E. Lehr, Ed., Academic Press, New York, N.Y., 1977, pp 110–191.
(2) For a recent review see H. D. Harzler in "Carbenes", R. A. Moss and M. Jones, Jr., Ed., Wiley-Interscience, New York, N.Y., 1975, pp 45–100.
(3) (a) C. Y. Lin and A. Krantz, *J. Chem. Soc., Chem. Commun.*, 1111 (1972); (b) A. Krantz, C. Y. Lin, and M. D. Newton, *J. Am. Chem. Soc.*, **95**, 2774 (1973); (c) O. L. Chapman, C. L. McIntosh, and J. Pacansky, *Ibid.*, **95**, 614 (1973); (d) O. L. Chapman, D. De La Cruz, R. Roth, and J. Pansky, *Ibid.*, **95**, 1337 (1973); (e) S. Masamune, M. Suda, H. Ona, and L. M. Leichter, *J. Chem. Soc., Chem. Commun.*, 1268 (1972); (f) G. Maier and B. Hoppe, *Tetrahedron Lett.*, 861 (1973).
(4) W. E. Billups, A. J. Blakeney, and W. T. Chamberlain, *J. Org. Chem.*, **41**, 3771 (1976).
(5) W. J. Hehre and J. A. Pople, *J. Am. Chem. Soc.*, **97**, 6941 (1970).
(6) P. S. Skell and J. H. Plonka, *J. Am. Chem. Soc.*, **92**, 836 (1970).
(7) S. Kammula and P. B. Shevlin, *J. Am. Chem. Soc.*, **96**, 7830 (1974).
(8) L. Friedman and H. Schecter, *J. Am. Chem. Soc.*, **82**, 1002 (1960).
(9) P. B. Shevlin and S. Kammula, *J. Am. Chem. Soc.*, **99**, 2627 (1977).
(10) Cyclobutenone was prepared by the method of J. B. Sieja, *J. Am. Chem. Soc.*, **93**, 130 (1971).
(11) F. Martinotti, M. J. Welch, and A. P. Wolf, *J. Chem. Soc. D*, 115 (1968).
(12) C. MacKay in "Carbenes", R. A. Moss and M. Jones, Jr., Ed., Wiley-Interscience, New York, N.Y., 1975, pp 1–42.
(13) L. Watts, J. D. Fitzpatrick, and R. Pettit, *J. Am. Chem. Soc.*, **88**, 623 (1966).
(14) P. B. Shevlin and A. P. Wolf, *J. Am. Chem. Soc.*, **92**, 406 (1970); H. W. Chang, A. Lautzenheiser and A. P. Wolf, *Tetrahedron Lett.*, 6295 (1966).
(15) R. C. Bingham, M. J. S. Dewar, and D. H. Lo, *J. Am. Chem. Soc.*, **97**, 2185, 1294, 1302, 1307 (1975).
(16) M. J. S. Dewar, H. Metiu, P. J. Student, A. Brown, R. C. Bingham, D. H. Lo, C. A. Ramsden, H. Kollmar, P. Weiner, and P. K. Bischof, "MINDO/3; Modified Intermediate Neglect of Differential Overlap", Program 279, Quantum Chemistry Program Exchange, Indiana University, 1975. In these calculations, all geometric parameters were optimized except the one defining the reaction coordinate.
(17) M. J. S. Dewar and H. W. Kollmar, *J. Am. Chem. Soc.*, **97**, 2933 (1974).
(18) W. J. Hehre, W. A. Latham, R. Ditchfield, M. D. Newton, and J. A. Pople, "Gaussian 70; *Ab Initio* SCF-MO Calculations on Organic Molecules", Program 236, Quantum Chemistry Program Exchange, Indiana University, 1975.
(19) R. S. Mulliken, *J. Chem. Phys.*, **23**, 1833 (1955).

Scott F. Dyer, Seetha Kammula, Philip B. Shevlin*
Department of Chemistry, Auburn University
Auburn, Alabama 36830
Received May 16, 1977

Species and Equilibria in the Methylmercury(II)–Imidazole System

Sir:

Although the acidity of the "pyrrole" nitrogen of metal-complexed imidazole and the subsequent reaction of the deprotonated pyrrole nitrogen as a ligand have been studied ex-

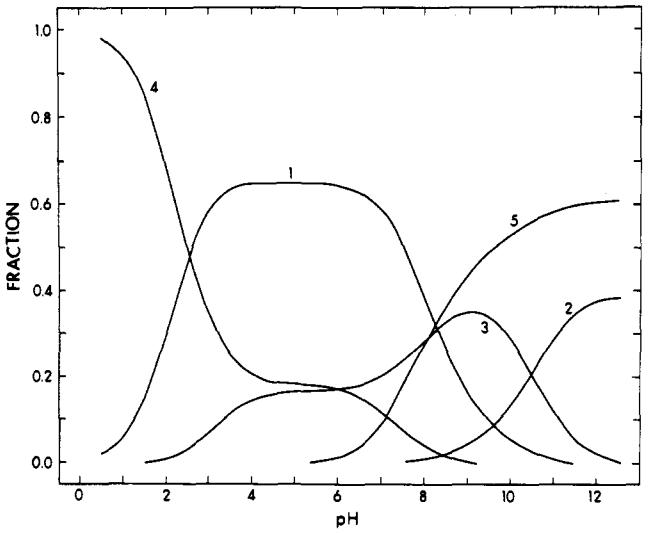

Figure 1. Fractional concentrations of the imidazole-containing species in a solution containing 0.01 M CH_3Hg^{II} and 0.01 M imidazole as a function of pH. Calculated from the equilibrium constants determined by NMR. Species are identified as **1**, CH_3HgHIm^+; **2**, CH_3HgIm; **3**, $(CH_3Hg)_2Im$; **4**, H_2Im^+; **5**, HIm.

tensively,[1] few quantitative results have been obtained because of insolubility of the polymeric imidazolato complexes and precipitation of the metals as their hydroxides. In this communication, we report the characterization of the methylmercury(II)–imidazole system over the pH range 1–13. Because the CH_3Hg^{II}–imidazole complexes are soluble and the CH_3Hg^{II} is unifunctional, it has been possible to characterize quantitatively the solution equilibria of a discrete dinuclear imidazolato complex for the first time.

Spectroscopic and potentiometric results indicate that complexes **1**–**3** form in aqueous solution.[2] The discrete mo-

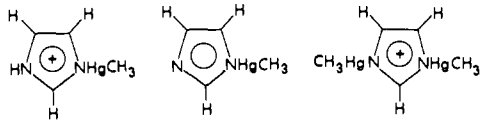

1 **2** **3**

lecular nature of complexes **2** and **3**, a consequence of the strong preference of CH_3Hg^+ for a coordination number of one,[3] is in marked contrast to the polymeric imidazolato complexes formed by other transition metals.[1] The formation of **1**–**3** can be described by the equilibria:

$$CH_3Hg^+ + HIm \overset{K_1}{\rightleftharpoons} CH_3HgHIm^+ \quad (1)$$

$$CH_3HgHIm^+ \overset{K_2}{\rightleftharpoons} CH_3HgIm + H^+ \quad (2)$$

$$CH_3Hg^+ + CH_3HgIm \overset{K_3}{\rightleftharpoons} (CH_3Hg)_2Im^+ \quad (3)$$

Formation constants determined independently from NMR chemical shift and pH titration experiments are listed in Table I. Also given are the equilibrium constant (K_4) for the formation of CH_3HgIm from CH_3Hg^+ and Im^-,[4] and the formation constant of the CH_3Hg^+–*N*-methylimidazole complex.

The results in Table I show that complexation of the "pyridine" nitrogen by CH_3Hg^+ causes a considerable increase in the acidity of the pyrrole nitrogen.[5] Also, there is a clear correlation between ligand basicity and the formation constants of the CH_3Hg^+ complexes, with both increasing in the order $HIm < CH_3HgIm < Im^-$. Because K_3 is larger than K_1, deprotonation of CH_3HgHIm^+ by increasing the pH gives rise

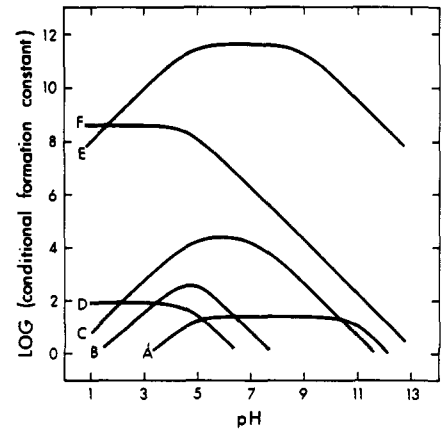

Figure 2. Log (conditional formation constants) vs. pH for methylmercury complexes of A, methylamine; B, acetic acid; C, *N*-methylimidazole; D, methionine (S); E, glutathione (S^-); F, iodide.

Table I. Equilibrium Constants for the Methylmercury(II)–Imidazole System

	NMR[a]	pH titration[b]
	Imidazole	
pK_A	7.13	7.10 ± 0.02
Log K_1	6.93 ± 0.04	7.14 ± 0.03
pK_2	9.61 ± 0.2	9.65 ± 0.1
Log K_3	8.26 ± 0.2	8.18 ± 0.1
Log K_4	11.76	11.79 ± 0.1
	N-Methylimidazole	
pK_A	7.18	
Log K_1	6.96	

[a] Ionic strength, 0.1–0.3 M, 25 °C. [b] Ionic strength, 0.1 M, 20 °C. For experimental details, see I. W. Erni, Dissertation, ETH, Zurich, 1977.

to free imidazole and the complex in which imidazolato bridges two CH_3Hg^{II} ions ($CH_3HgHIm^+ + CH_3HgIm \rightleftharpoons (CH_3Hg)_2Im^+ + HIm$). The equilibrium constant for this reaction is K_3/K_1. Because of competing acid–base equilibria, the extent to which complexes **1**–**3** form is pH dependent, as shown by the fractional concentration curves in Figure 1.

The binding of CH_3Hg^{II} by the functional groups of proteins is of interest because of the involvement of such binding in methylmercury poisoning and the use of CH_3Hg^{II} as a titrant for protein sulfhydryl groups. If we can assume that formation constants of CH_3Hg^{II} complexes of model ligands can be extrapolated to its binding by protein functional groups,[6] we can predict the order in which the various binding sites combine with CH_3Hg^{II}. Formation constants for the complexes of a representative series of ligands increase in the order[7] methionine (S) < acetic acid < *N*-methylimidazole < methylamine < glutathione (S^-). Conclusions based on formation constants are misleading, however, if competing protonation and hydroxide-complexation equilibria are not considered. These competing equilibria can be most easily accounted for by using conditional formation constants, which for the above series of ligands are given as a function of pH in Figure 2. The conditional formation constant curve for CH_3HgI is also plotted in Figure 2.

The conditional formation constants indicate that sulfhydryl groups are clearly the most important CH_3Hg^{II} binding sites in proteins, but that imidazole also has a surprisingly large relative affinity for CH_3Hg^{II}. The relative positions of the conditional formation constants are in accord with the use of CH_3HgI as a selective titrant for protein sulfhydryl groups. Presumably, binding of CH_3Hg^{II} by peptide and protein imidazole groups also will be accompanied by an increase in the

acidity of the proton bound to the pyrrole nitrogen and the formation of dinuclear imidazolato complexes. Studies on the binding of CH_3Hg^{II} by histidyl residues of peptides and proteins are in progress.

Acknowledgments. This research was supported in part by the National Research Council of Canada and the Swiss National Science Foundation.

Reference and Notes

(1) R. J. Sundberg and R. B. Martin, *Chem. Rev.*, **74**, 471 (1974).
(2) Complexes 1–3 have been isolated from aqueous solution, and their compositions and structural formulas have been established by elemental analysis and NMR and Raman spectroscopy.
(3) G. Schwarzenbach and M. Schellenberg, *Helv. Chim. Acta*, **48**, 28 (1965). However, vibrational spectra of crystalline CH_3HgIm provide evidence for intermolecular bonding, presumably involving the free nitrogen atom.
(4) (a) K_4 was calculated from K_1, K_2, and the pK_A of the pyrrole nitrogen of Him. For the NMR experiments, a pK_A of 14.44 was used;[4b] in the pH titration experiments, a pK_A of 14.3 was used.[4c] (b) P. George, G. I. H. Hananla, D. H. Irvine, and I. Abu-Issa, *J. Chem. Soc.*, 5689 (1964). (c) G. Geier and I. Erni, unpublished results.
(5) (a) For comparison, the pK_A of the imidazole complex of aquocobalamin is 10.25[5b] and that of the imidazole in $(NH_3)_5CoHim^{+}$ is 10.02.[5c] (b) G. I. H. Hananla and D. H. Irvine, *J. Chem. Soc.*, 5694 (1964). (c) J. Harrowfield, V. Norris, and A. M. Sargeson, *J. Am. Chem. Soc.*, **98**, 7282 (1976).
(6) This is expected to be a good assumption because of the pronounced preference of CH_3Hg^{II} for a coordination number of one.
(7) M. T. Fairhurst and D. L. Rabenstein, *Inorg. Chem.*, **14**, 1413 (1975), and references cited therein.

Christopher A. Evans, Dallas L. Rabenstein*
Department of Chemistry, University of Alberta
Edmonton, Canada

Gerhard Geier,* Isidor W. Erni
Laboratorium für Anorganische Chemie
Eidgenossiche Technische Hochschule
8092 Zurich, Switzerland

Recieved June 17, 1977

Direct Calculation of the Equilibrium Value of the Energy of Activation for Dissociation of H_2 by Ar and Evidence for the Important Contribution of Collisional Dissociation from Low Vibrational Quantum Numbers and High Rotational Quantum Numbers at Shock Tube Temperatures

Sir:

Although dissociation of diatomic molecules under high-temperature steady-state conditions has been studied for over 20 years, the detailed interpretation of the results is still controversial. Two particularly important unresolved questions are the following.[1-3] (i) Why is the Arrhenius energy of activation E_a, defined by

$$E_a = -R \frac{d \ln k_d(T)}{d(1/T)} \quad (1)$$

where $k_d(T)$ is the observed steady-state dissociation rate coefficient, much less (6 or more kcal mol^{-1} for typical systems) than the bond dissociation energy D_0? (ii) Does dissociation proceed only or primarily from the topmost vibrational level (ladder climbing) or do lower vibrational levels make important contributions? These questions are complicated because it is necessary to consider the competition of energy transfer and dissociation which may result in a highly nonequilibrium population of the highest energy levels during the steady-state reaction.[1-4] It has usually been assumed that, if all states could be kept at equilibrium, dissociation would proceed primarily from the topmost vibrational energy level and E_a would be significantly higher than observed. Attempts to understand the mechanism of the dissociation process have been hampered by the lack of accurate knowledge of the state-to-state transition rate coefficients.[1-5] Some workers[6,7] have used the classical trajectory method to study the dissociation process. Here we report a quasi-classical trajectory study[8,9] of the relative contribution to the dissociation rate of collisions with various initial vibrational quantum numbers v of para-H_2 dilute in Ar under conditions of local equilibrium of reactants[10] at 4500 K. We find large contributions from low v. Since vibrational nonequilibrium effects will tend to decrease the relative contribution of high-v collisions, this implies even larger contributions from low-v collisions for a rotationally equilibrated, vibrationally nonequilibrated steady state.[11] In addition we calculate that E_a at equilibrium is 6 kcal mol^{-1} below D_0. Thus it is not necessary to invoke nonequilibrium effects solely because D_0 considerably exceeds E_a.[12]

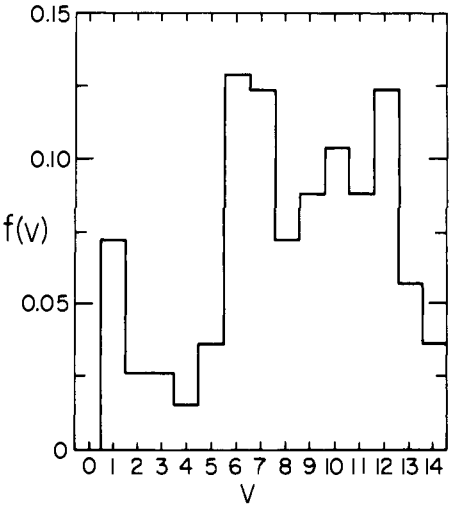

Figure 1. Calculated distribution of reactive collisions for the reaction Ar + $H_2(v)$ → Ar + H + H at local equilibrium of reactants at 4500 K sorted according to initial vibrational quantum number v.

Our general methods and many other references are given elsewhere.[9] We used our own full potential surface,[9] which is the most accurate available. States of negative internal energy (compared with the separated-atom limit) are considered to be reactant states; quasi-bound H_2 and dissociated H_2 are considered to be product states.[13] We calculated 11 180 trajectories with maximum impact parameter 3.2 Å and with total energy in excess of the dissociation threshold but otherwise randomly sampled at 4500 K. We evaluated the equilibrium E_a by the Tolman definition,[14] i.e., at local equilibrium E_a is the average total energy of pairs that react minus that for all pairs. The result is $E_a = 97.2 \pm 1.0$ kcal mol^{-1} (68% confidence limits). The critically evaluated 1972 recommended experimental value[15] (experiments involved normal H_2) is 96 ± 4 kcal mol^{-1} and a more recent experimental value[16] is 89 kcal mol^{-1}. Since D_0 is 103.3 kcal mol^{-1}, a large negative deviation of E_a from D_0 is predicted even under local equilibrium conditions. The local-equilibrium rate coefficient is calculated to be 1.3 (±0.1) × 10^{-13} cm^3 molecules^{-1} s^{-1} (68% confidence limits) compared with experimental values of[15] $8(^{+8}_{-4}) \times 10^{-15}$ cm^3 molecules^{-1} s^{-1} and[16] 7.5×10^{-15} cm^3 molecules^{-1} s^{-1}. Thus the calculated local-equilibrium rate coefficient is larger than the observed rate coefficient. Nonequilibrium effects are expected[1-3,6,17] to decrease the rate.

Figure 1 shows the fraction $f(v)$ of reacting trajectories with each initial v; it shows 30% of the reaction comes from v = 1–6, 48% from v = 7–11, and only 22% from v = 12–14. For the typical v, the relative uncertainty in the histogram height due to the finite Monte Carlo sampling size is 28% (68% confi-